Hindawi
Material Design & Processing Communications
Volume 2022, Article ID 5056057, 13 pages
https://doi.org/10.1155/2022/5056057

Research Article

Gear Tooth Root Bending Strength Estimation under the Assumption of Fatigue Limit Existence

Luca Bonaiti and Carlo Gorla

Politecnico di Milano, Dipartimento di Meccanica, Via La Masa 1, Milano 20156, Italy

Correspondence should be addressed to Luca Bonaiti; luca.bonaiti@polimi.it

Received 17 March 2022; Revised 25 April 2022; Accepted 26 April 2022; Published 1 June 2022

Academic Editor: Enrico Salvati

Being able to properly predict gear failure is a key aspect to achieve a reliable light-weight gearbox. Among the several gear failures, tooth root bending fatigue is considered as the most dangerous one because it implies the stoppage of the whole gearbox. In order to characterize a gear for this phenomena, Single Tooth Bending Fatigue (STBF) tests are the most performed ones. However, as in STBF test THERE IS no sliding/rolling contact and as the specimens are teeth rather than gears, some differences occur between the test conditions and those of the real case. This paper deals with the statistical ones that is the estimation of the gear SN curve starting from the teeth one. The teeth SN curve has been estimated by means of a statistical model developed considering Murakami's idea of nonpropagating crack. Then, a methodology based on statistic of extreme is adopted for the purpose of estimating the gear SN curve.

1. Introduction

Gears are mechanical components that, through the meshing of profiles, transmit power between two axes with an almost constant angular speed ratio [1, 2]. Due to their peculiar working principles, several failure mechanisms may occur in gear. Both ISO/FDIS 10825-1 [3] and ANSI/AGMA 1010-F14 [4] enlist several failure mechanisms that can affect gears. ISO/FDIS 10825-1 [3] classifies the most classical failure mode within two main macrocategories: tribological damages (i.e., scuffing and wear) and fatigue damages (i.e., contact fatigue and bending fatigue). In the design phase, several analytical calculation methods are adopted in order to avoid those damage phenomena (e.g., ISO 6336 series). Furthermore, during the exercise, it is possible to rely on monitoring technique as a means to control the advancement of the aforementioned phenomena (e.g. [5–9]).

On the one hand, scuffing, wear, and contact fatigue are generated by the rolling-sliding loaded contact between tooth flanks. On the other hand, the tooth root bending fatigue phenomenon is generated by the normal force that, during gear meshing, varies both in terms of load entity (due to the load sharing between teeth) and position (as the contact point moves along tooth active profile). As a result, the stress occurring within the tooth root is not constant, but it varies between a very small negative value (due to the extension of the stress field of the tooth root adjacent field), to a maximum (at the outer point of single tooth in contact). Furthermore, the tooth root itself implies the presence of a notch, which implies very high stress values [10, 11].

Among all gear failure modes, designers consider the tooth root bending fatigue failure mode as the most dangerous one. Indeed, the failure of a single tooth root implies a sudden stoppage of the power flow within the gearbox; thus, it is no more able to operate.

In order to avoid the tooth root bending fatigue failure, designers rely on several standardized calculation methods (e.g. ISO 6336-3 [12] and ANSI/AGMA 2001 [13]). According to them, a gear pair is assessed by comparing the tooth root stress with the limit value for the desired life. Moreover, adopting the classical damage accumulation framework provided by the Palmgren-Miner rule, both ISO 6336-3 [12]

(together with ISO 6336-6 [14]) and ANSI/AGMA 2001 [13] allow designers to perform a load spectra analysis within the classical gear assessment framework.

Apart from the knowledge of the load spectra, any damage accumulation framework requires also the knowledge of the component SN curve. Both ISO 6336-5 [15] and ANSI/AGMA 2001 [13] propose typical endurance limit that, together with corrective coefficients (i.e., Y_{NT} for ISO 6336-3 [12] and Y_N for ANSI/AGMA 2001 [13]), defines the gear SN curve. It is worth mentioning that the same concept is applied for the macropitting case too.

Figure 1 shows the typical dimensionless SN curve for several typical gear material proposed by ISO 6336-3 [12]. On the one hand, the static and the limited life region are well defined. On the other hand, the long life region is represented by a shaded area whose limits are an inclined line (that implies the inexistence of the fatigue limit) and a horizontal one (representing the gear fatigue limit). Nevertheless, ANSI/AGMA 2001 [13] proposes a slightly different curve where there is not a fatigue limit, but two inclined lines. All those curves are defined at 1% gear failure probability. Different reliability levels can be adopted by embracing further coefficients that shift the SN curve. ANSI/AGMA 2001 [13] includes this kind of coefficient while designers adopting ISO 6336 series can adopt those suggested by Hein et al. [16]. Nevertheless, both ANSI/AGMA 2001 [13] and ISO 6336 series strongly encourage to perform specific experimental campaign in order to estimate the gear SN curve.

This paper is aimed at discussing how to elaborate tooth root bending fatigue data in order to being able to estimate the component SN curve. Here, a statistical framework through which analyse gear fatigue data is discussed and adopted in order to estimate the gear SN curve. Finally, results are compared with the ones obtained with other literature data.

This article is aimed at continuing some previous works of the authors [17, 18]. There, the statistical framework is based on [19, 20], where a curve without fatigue limit is proposed. Nevertheless, the existence or not of the fatigue limit is sill under discussion (e.g. [21, 22]). Therefore, the proposed statistical framework features the presence of the fatigue limit.

The rationale behind this choice is that recent development in tooth root bending fatigue characterization [23–27] suggests that Murakami's idea of nonpropagating cracks (e.g., [28–30]) can be apply also in the case of tooth root bending fatigue (thus, the gear tooth root bending phenomena can be modelled considering the existence of the fatigue limit). Among several models to describe the fatigue behaviour of a component (e.g., [19, 31, 32]), an SN parameter estimation technique, developed by Loren, S. [33, 34], also based on Murakami's idea of nonpropagating cracks, is adopted as a means to estimate the specimen SN curve.

2. Gear Testing for Tooth Root Bending Fatigue

ISO 6336-5: 2016 [15] presents four different methodologies for tooth root bending fatigue testing. Method A refers to test performed on gears, whose dimension and loading conditions are as close as possible to the actual case. Method B describes those tests performed on reference gears, whose dimensions and loading conditions differ from the actual one; Single Tooth Bending Fatigue Test (STBF) (also called pulsator test), which will be described later, belongs to this category. Methods B_k and B_p denote test conducted on notched and unnotched uniaxial specimen, respectively. Gear testing literature respects those categories. Indeed, it is possible to find test performed on rotating gears (e.g., [25, 35–37]), by means of the STBF procedure (e.g. [25, 26, 36–42]) as well as test performed on notched specimen (e.g. [43–45]).

The STBF procedure seems to be the most adopted tooth root bending fatigue testing methodologies. Indeed, as mentioned by McPherson and Rao [46], the STBF testing procedure has several advantages. Firstly, STBF tests can be performed on any uniaxial testing machine. Secondly, as there is no rolling/sliding contact, only the tooth root bending fatigue failure mode is present. Therefore, it is possible to perform tooth root bending fatigue test without the risk of falling into other gear failure modes (e.g., scuffing). Finally, by testing teeth rather than directly the gear, it is possible to obtain more specimen from the same component.

STBF tests replicate the tooth root bending phenomena by applying, by means of two anvils, a force far away from the tooth root. Two are the configuration typically adopted in order to perform STBF test. The first one is the symmetric configuration, in which two anvils apply the load on the teeth flanks. Typically, the anvil spans over 3/5 teeth, and thanks to the same principle of the Wildhaber measurements [47], the contact between anvils and teeth flanks occurs at the same nominal diameter. Hence, both teeth result to be subject to the same nominal tooth root stress. The latter configuration is the asymmetric one, deeply described in [48, 49]. Here, the machine load is directly only one tooth, while a second tooth, together with a centring pin, works as supports, reacting to the machine load. Therefore, only one tooth is tested at the time. Both test configurations must keep a minimum compressive force with a view to maintain the specimen in position.

As test data are evaluated according to the force applied by the test rig (i.e., a mechanical pulsator in this case) on the gear teeth, in order to move STBF force data into meshing gear tooth root stress, any approaches that to translate STBF experimental points to running gears have to deal with different passages:

(1) Calculate the STBF tooth root stress. This is typically realized by means of FEM (e.g., [50, 51]) or using analytical methods (e.g., ISO 6336-3 method B [12])

(2) Calculate the teeth SN curve in meshing gear condition starting from the teeth STBF data points

(3) Define the gear SN curve, in meshing gear condition, at the proper failure probability level (e.g., 1%)

However, the advantages of the STBF testing procedure imply that two differences arise between the STBF loading

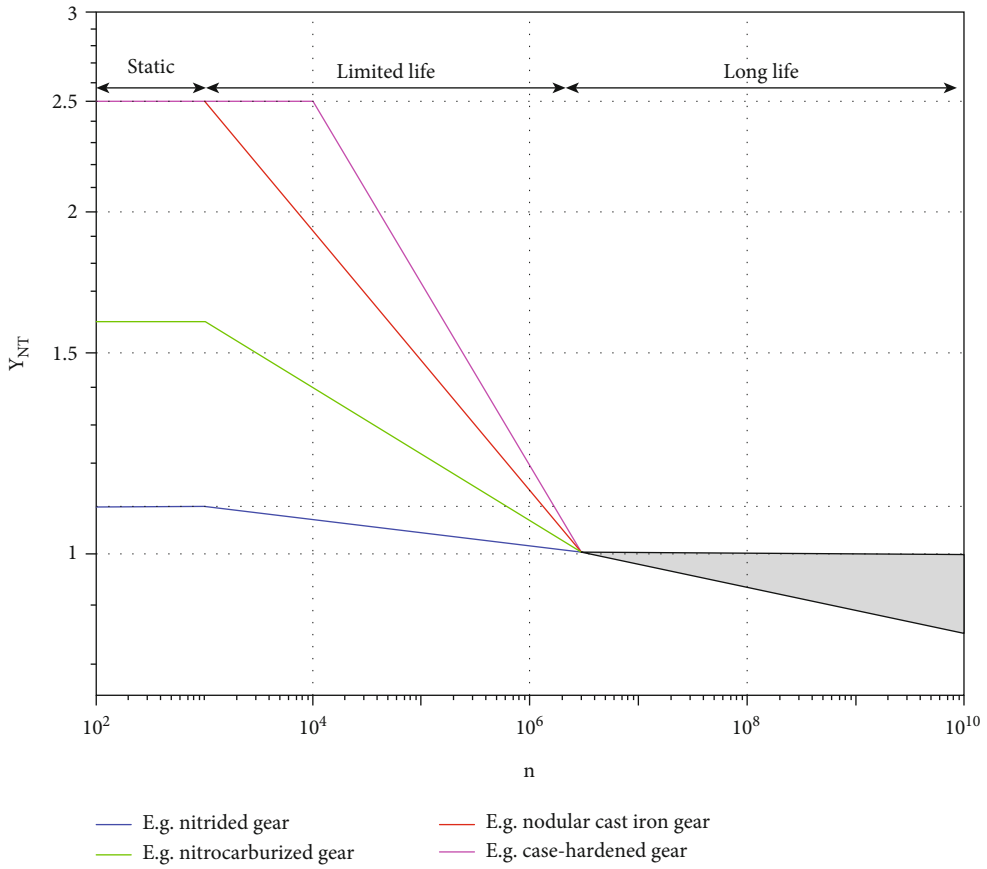

Figure 1: Typical SN curve according to ISO 6336 [12].

case and the actual case [23, 36–39, 52, 53]. On the one hand, the lack of the rolling/sliding condition implies that the loading condition occurring within the toot root is different [11, 54, 55]. On the other hand, the fact that the tests are performed on the teeth rather that gear implies a statistical difference [17, 18]. Therefore, the results of STBF test have to be corrected in order to be used for the assessment of a gear pair under the real case loading scenario. Four different approaches can be found in literature, one developed by Seabrook and Dudley [53], the FVA report no. 304 [39], the work of Rao and McPherson [36, 37], and, recently, the one proposed by Hong et. al. [52]. Interested readers are referred to [17, 52] for a comprehensive review about how the literature deals with the aforementioned passages.

The authors [17, 18] adopt statistic of extreme in order to address the statistical difference while high-cycle multiaxial fatigue criteria (coupled with numerical simulations) are adopted to address the problem of the different loading conditions by defining a coefficient $f_{korr,FEM}$ [11]. The same is applied here.

In the last twenty years, the authors have adopted a symmetric STBF procedure for the estimation of the tooth root bending fatigue resistance on several types of gears material/geometry. Some examples: austenite ductile iron gears [56], aeronautical-grade materials [50, 51], gears with very large modulus [57, 58] and 17-4 PH additively manufactured gears [59, 60]. All of them have been performed on a Schenck pulsator. For each experimental campaign, a specific equipment, whose features depend on the examined gear specimen, has been designed and adopted. Figure 2 shows the equipment adopted for the present experimental campaign. In order to maintain the gear specimen in position, a load ratio R=0.1 has been adopted. For additional details regarding the adopted testing procedure, the interested reader can refer to the aforementioned references. Result data discussed in [11, 17, 18, 61] are adopted here as reference case.

3. Estimation of the Specimen SN Curve

Under the assumption of fatigue limit existence, when estimating the fatigue behaviour of a component/specimen, both the finite life and the infinite life are considered as two random variables, typically assumed to follow a log-normal distribution:

$$\begin{cases} y_{(x_i)} = \ln(n_i) \sim N\left(\nu_{(x_i)}, \sigma_{\nu(x_i)}{}^2\right), \\ x_{e_i} = \ln\left(S_{e_i}\right) \sim N\left(\mu_{x_e}, \sigma_{x_e}{}^2\right), \end{cases} \quad (1)$$

where the terms x and y refer to the logarithm of the applied stress S and the number of cycle n, respectively. $y_{(x_i)}$ is a normally distributed random variable, whose mean $\nu_{(x_i)}$

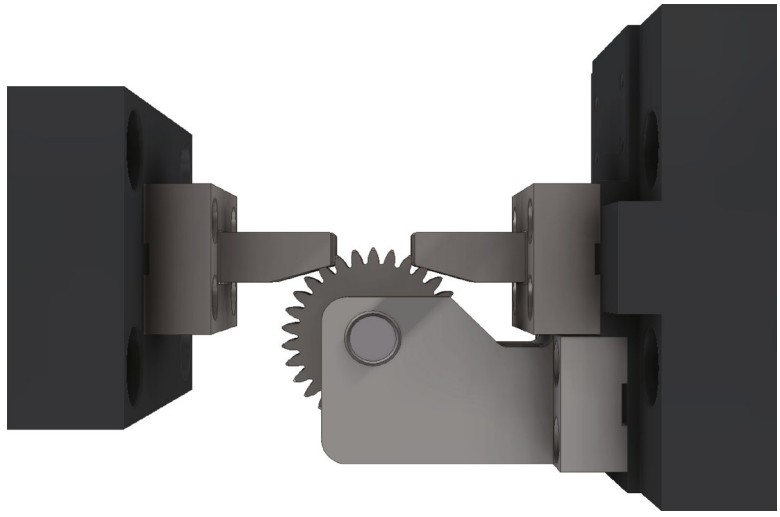

Figure 2: Adopted STBF test equipment.

depends on the applied stress. Also, the variance $\sigma_{v(x_i)}$ can be described as dependent on the applied stress too [32, 62].

Finite life implies that the higher the stress, the lower will be the number of cycles to failure. Therefore, $v_{(x_i)}$ can be any decreasing continuous function. Following Basquin's approximation of the SN curve, $v_{(x_i)}$ can be a linear one. The same is adopted here. The variance $\sigma_{v(x_i)}{}^2$ is considered as constant. On the other hand, infinite life (i.e., the long life region) implies that there is a stress S_∞ below which the component has an infinite life (i.e., the fatigue limit). μ_{x_e} and $\sigma_{x_e}{}^2$ are S_∞ mean and variance.

Therefore, Equation (1) can be rewritten as follows:

$$\begin{cases} y_{(x_i)} = \ln\left(n_i\right) \sim N\left(a + bx_i, \sigma_n{}^2\right), \\ x_{e_i} = \ln\left(S_{e_i}\right) \sim N\left(\mu_{x_e}, \sigma_{x_e}{}^2\right), \end{cases} \tag{2}$$

where a and b are the parameter describing the linear relationship between x_i (i.e., the log of the applied stress) and y_i (i.e., the log of the number of cycles).

A first attempt to estimate a component/specimen SN curve can be accomplished by investigating the two regions separately; defining two different sets of experimental data, each one adopted to estimate a single region. The finite life region behaviour is estimated performing test at high load levels. On the other hand, the fatigue limit can be estimated adopting a staircase procedure.

However, despite being relatively easy, this procedure has two main disadvantages:

(1) The whole SN curve is biased by how the points have been collected. Point defined while investigating the infinite life can be adopted to describe the finite life behaviour. On the other hand, points obtained while looking into the finite life provide also information about the infinite life region

(2) The staircase procedure is a sensitivity analysis aimed to estimate an endurance limit that is the load required to have 50% of failure at a certain lifetime (i.e., the runout level). On the other hand, the fatigue limit is the load level under which 50% of the tested component will show infinite life. The endurance limit can describe the fatigue one only if the runout threshold is sufficiently high

Surely, it would be better to adopt an SN curve estimation procedure that is able to estimate both finite and infinite life within the same calculation procedure. Therefore, a framework is able to overcome the below disadvantages while still working with a runout level n_{RO}. Fatigue literature presents several models able that satisfy the aforementioned requirement (e.g., [31]). Among them, the model proposed by Loren [33, 34] is adopted here. This model has been preferred in respect to the random fatigue limit (RFL) as it lays its basis on both statistical and experimental evidences, while the RFL [31] as the Loren's model lays its basis on both statistical and experimental evidence, while the RFL is based only on statistical consideration.

The model proposed by Loren, S. [33, 34] is based on Murakami's idea of nonpropagating cracks, which suggests that the limited life and the fatigue limit are related to two different phenomena (e.g., [28–30]). In the region ahead the fatigue knee (i.e., the limited life region), the cracks nucleate, and then, they propagate until the component/specimen breakage. On the other hand, in the region after the fatigue knee (i.e., the long life region), cracks can nucleate but their propagation stop (if the stress level is below the fatigue limit). Experimental evidence confirms that also tooth root bending fatigue follows Murakami's idea of nonpropagating cracks [23–27].

Loren, S. model [33] works within a Maximum Likelihood (ML) framework, which is a technique to estimate distribution parameters based on the idea of finding, mathematically, those parameters that are more likely to represent the data. More precisely, the estimated distribution parameters are those that maximize the likelihood $\mathscr{L}$, which

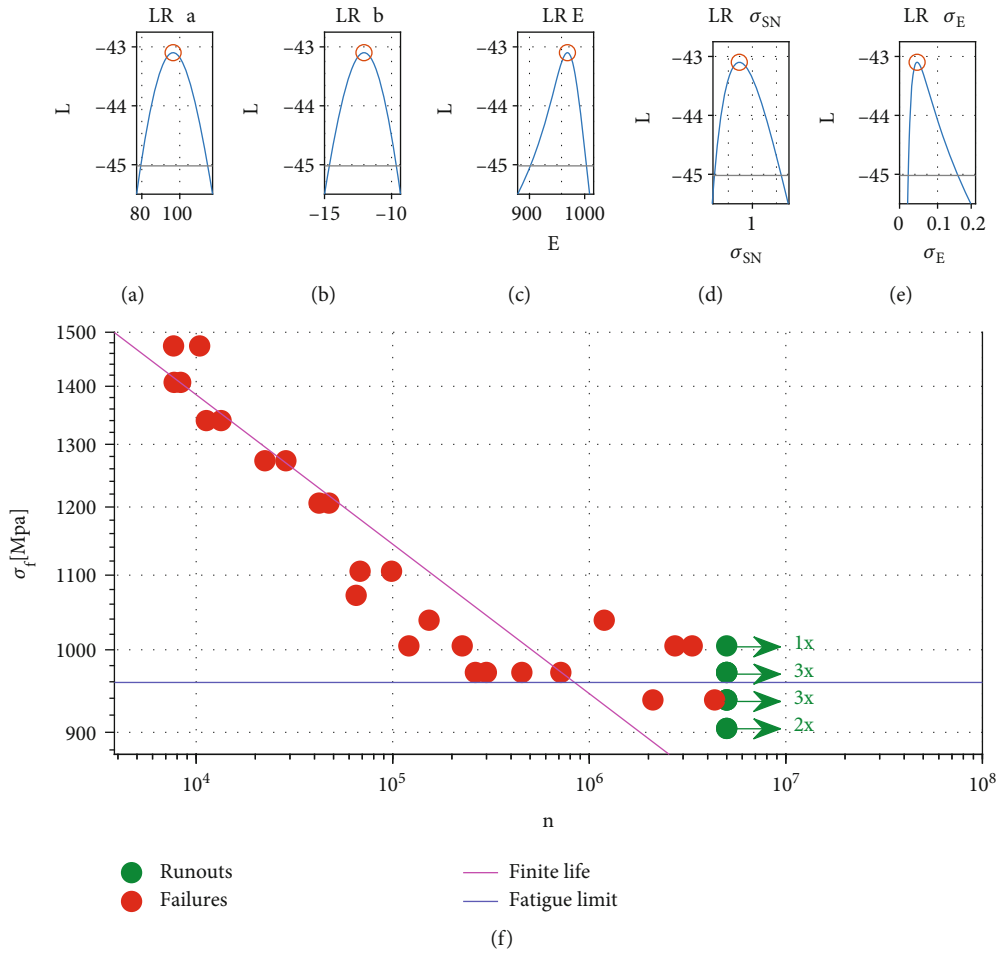

FIGURE 3: Estimated model parameter. Their likelihood ratio profile is shown in (a–e). On the other hand, the relation between the estimated finite life and experimental points is shown in (f).

is based on the probability of observing the data. For further details concerning the ML estimation as well as likelihood properties, the interested reader is referred to [62–64].

According to Loren, S. [33], the i^{th} component/specimen may have failed because the stress level is above the stress limit and/or it belongs to the finite live region. $\mathscr{L}_{F,i}$, i.e., the likelihood function for an observed value (i.e., a failure), is defined as follows:

$$\mathscr{L}_{F,i} = f_{\left(y_{(x_i)};a+bx_i,\sigma_n^2\right)} dy\, F_{(x_i;E,\sigma_E^2)}, \tag{3}$$

where the symbol $f_{(\ldots)}$ refers to a probability density function (PDF) while $F_{(\ldots)}$ refers to a cumulative density function (CDF).

On the other hand, the i^{th} component/specimen may present a life above the runout level n_{RO} for two reasons: at the stress level, it has a finite life n_i above n_{RO} or the stress level is below S_∞. $\mathscr{L}_{C,i}$, i.e., likelihood for a right-hand censored (i.e., a survival) data, is as follows:

$$\mathscr{L}_{C,i} = 1 - \left(F_{\left(y_{(x_i)};a+bx_i,\sigma_n^2\right)}\, F_{(x_i;E,\sigma_E^2)}\right). \tag{4}$$

It is worth mentioning that, due to the compresence of the two phenomena, both Equation (3) and Equation (4) present terms related to the two different PDFs/CDFs.

The two likelihood terms are combined in the likelihood $\mathscr{L}$:

$$\mathscr{L} = \prod_{i=1}^{n} \left(\mathscr{L}_{F,i}\right)^{\delta_i} \prod_{i=1}^{n} \left(\mathscr{L}_{C,i}\right)^{1-\delta_i}, \tag{5}$$

where δ_i is equal to 1 for observed data and equal to zero for censored data.

However, in order to perform the calculation procedure, it is more common to work on the log likelihood l, that is the natural logarithm of the likelihood $\mathscr{L}$:

$$l = \ln\left(\mathscr{L}\right) = \delta_i \sum_{1=1}^{n} \ln(\mathscr{L}_{F,i}) + (1-\delta_i) \sum_{1=1}^{n} \ln(\mathscr{L}_{C,i}). \tag{6}$$

Equation (3) and Equation (4) are then included in Equation (6), thus obtaining the final log-likelihood

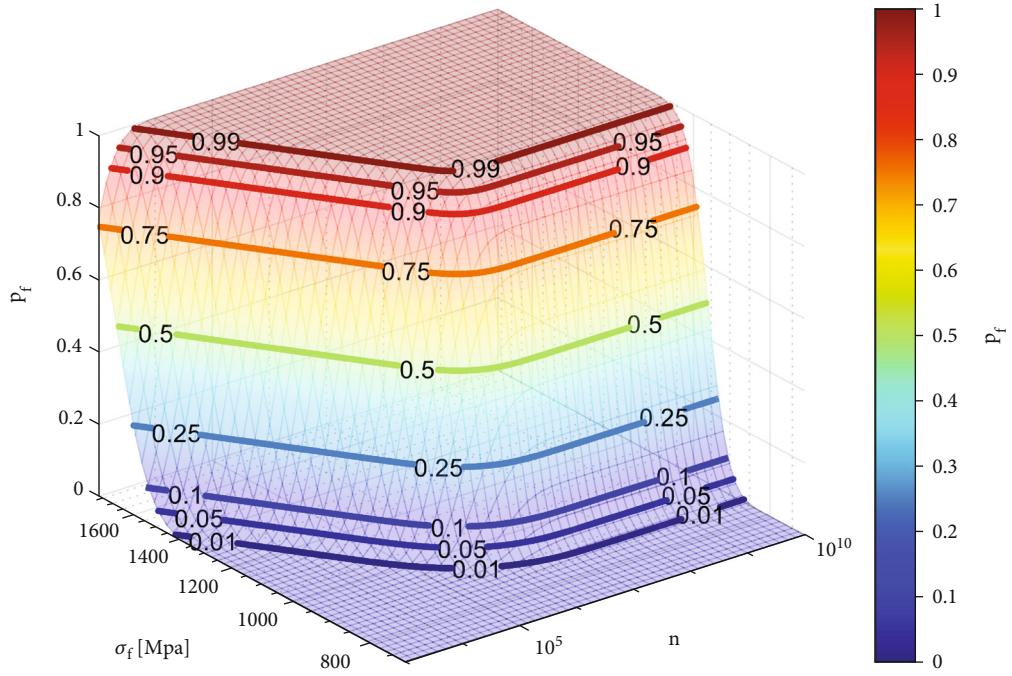

Figure 4: Estimated teeth PSN surface.

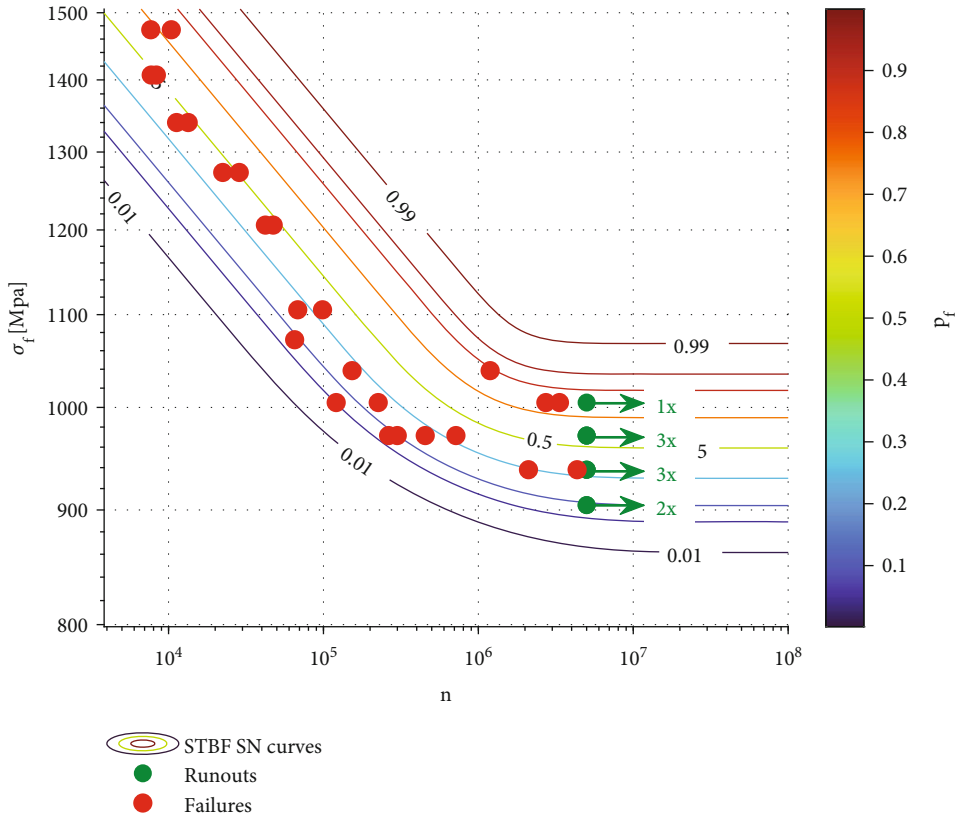

Figure 5: Estimated STBF SN curve and experimental data. The estimated teeth CDF is shown through curves at the same probability of failure.

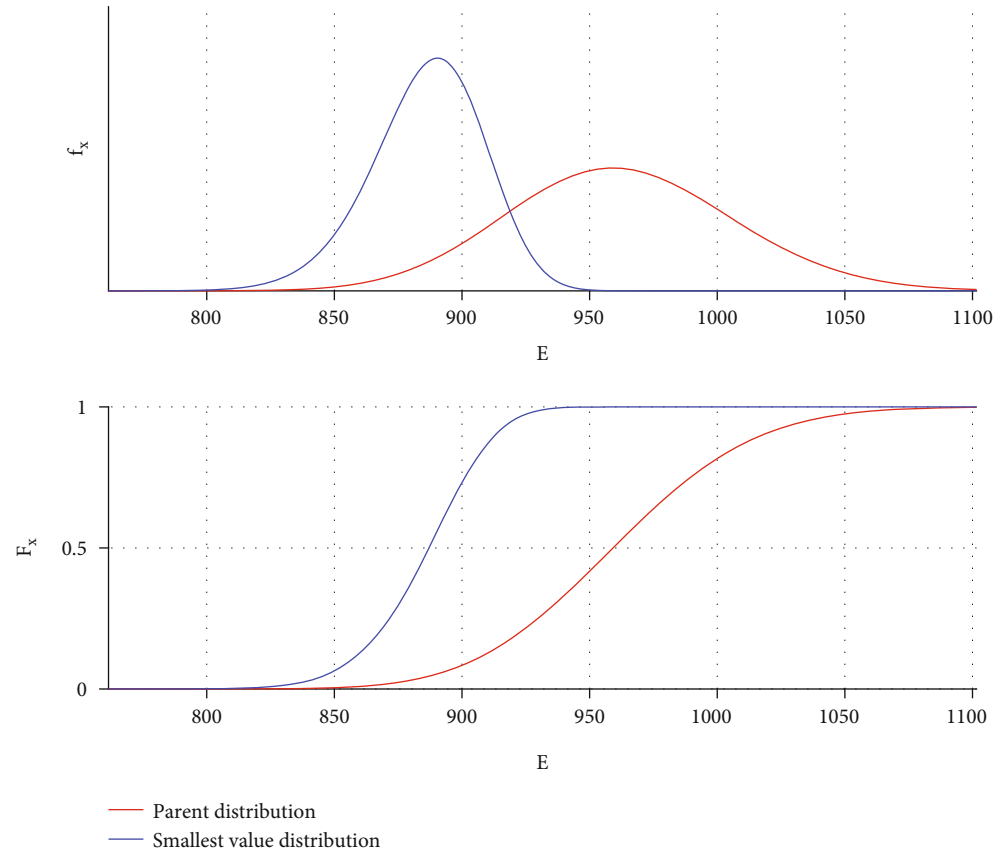

FIGURE 6: From parent to smallest extreme value distribution. The example is based on the estimated $F_{(x_i;E,\sigma_{E^2})}$ and the actual number of teeth pair.

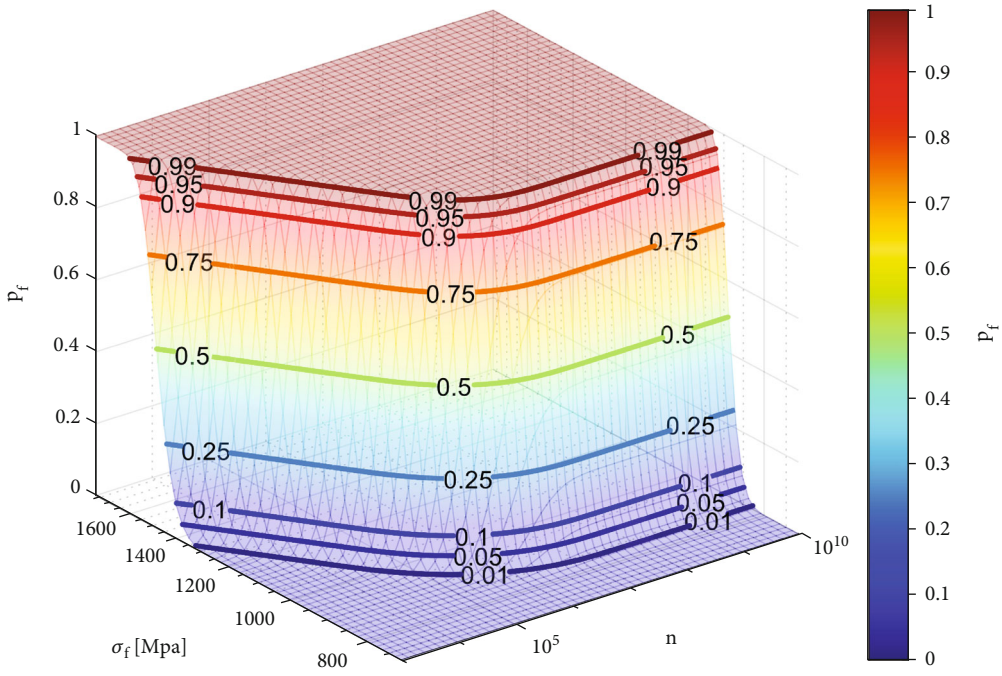

FIGURE 7: Estimated gear PSN curve.

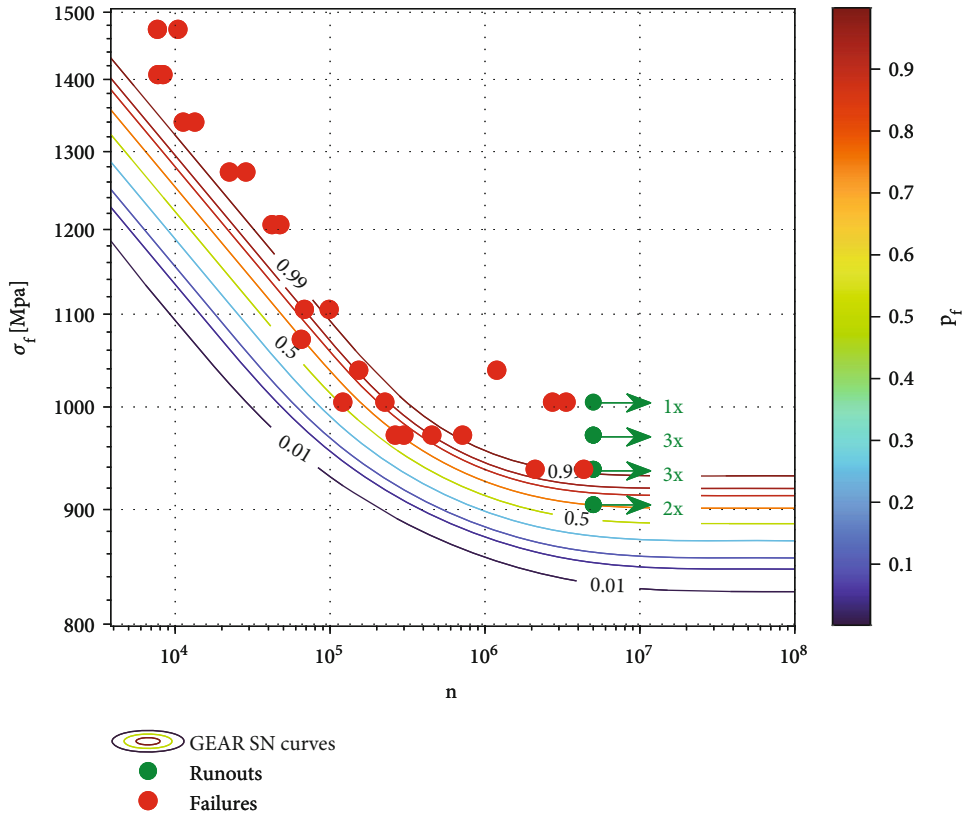

FIGURE 8: Estimated gear SN curve and experimental data. The estimated gear CDF is shown through curves at the same probability of failure.

formulation:

$$l = \delta_i \sum_{1=1}^{n} \ln\left(\varphi_{\left(y_{(x_i)};a+bx_i,\sigma_n{}^2\right)} dy\, \phi_{\left(x_i;E,\sigma_E{}^2\right)}\right) + n \ln(dy) + (1-\delta_i) \sum_{1=1}^{n} \ln\left(1 - \left(\phi_{\left(y_{(x_i)};a+bx_i,\sigma_n{}^2\right)} \phi_{\left(x_i;E,\sigma_E{}^2\right)}\right)\right). \quad (7)$$

The parameters that are estimate by ML are those that maximize l and, subsequently, also $\mathscr{L}$. However, as the classical calculation software includes only minimization algorithm, those parameters are obtained by minimizing $-l$. The term $n \ln(dy)$ is a constant term that is removed from the calculation procedure.

Figure 3 reports the estimated model parameters and how they interact with the experimental data. By expressing each parameter within its confidence interval, likelihood ratio (LR) has been used in order to verify the model assumption [62, 63, 65].

As two separate failure mechanisms are present, the PDF/CDF representing the failure probability of the specimen/component is described by the combination of both finite life and infinite life PDFs/CDFs [34]:

$$F = F_{\left(y_{(x_i)};a+bx_i,\sigma_n{}^2\right)}\, F_{\left(x_i;E,\sigma_E{}^2\right)}. \quad (8)$$

Different curve, at different failure rate, can be obtained by calculating, for different level, the number of cycles of the corresponding percentile. Furthermore, Equation (8) allows to calculate the probability of observing a failure after n number of cycle when the specimen/component is subject to a certain stress level. This 3D surface is the so-called PSN curve. Figure 4 report the estimated teeth PSN curve. Similarly, Figure 5 shows different SN, at different reliability level.

The experimental data discussed here have been obtained adopting a symmetric STBF. Therefore, each experimental point represents two teeth, which have been tested at the same time at the same nominal load. This implies that each experimental points contains information about both the tested teeth. On the one hand, if one teeth fails after n cycles, the other one shows a life that is greater than n, and if the test stops because n_{RO} has been reached, both teeth shows a life greater than n_{RO}. If one focuses on the information provided by each single tooth, data are subject to randomly right censoring, i.e., there is no a fixed value after which teeth testing is stopped. Indeed, the test of a single teeth results to be stopped both due to tooth failures after n cycles (which is random) or for having reached the runout level. On the other hand, if the focus is on the STBF test point, the test is stopped only because the runout level has been reached.

Within [17, 18], the adopted model allows the usage randomly right censored data. Therefore, it has been possible to estimate the SN curve referred to one single tooth. However, within [33, 34], there is no mention whereas it is possible to use randomly right censored data. Therefore, the estimation

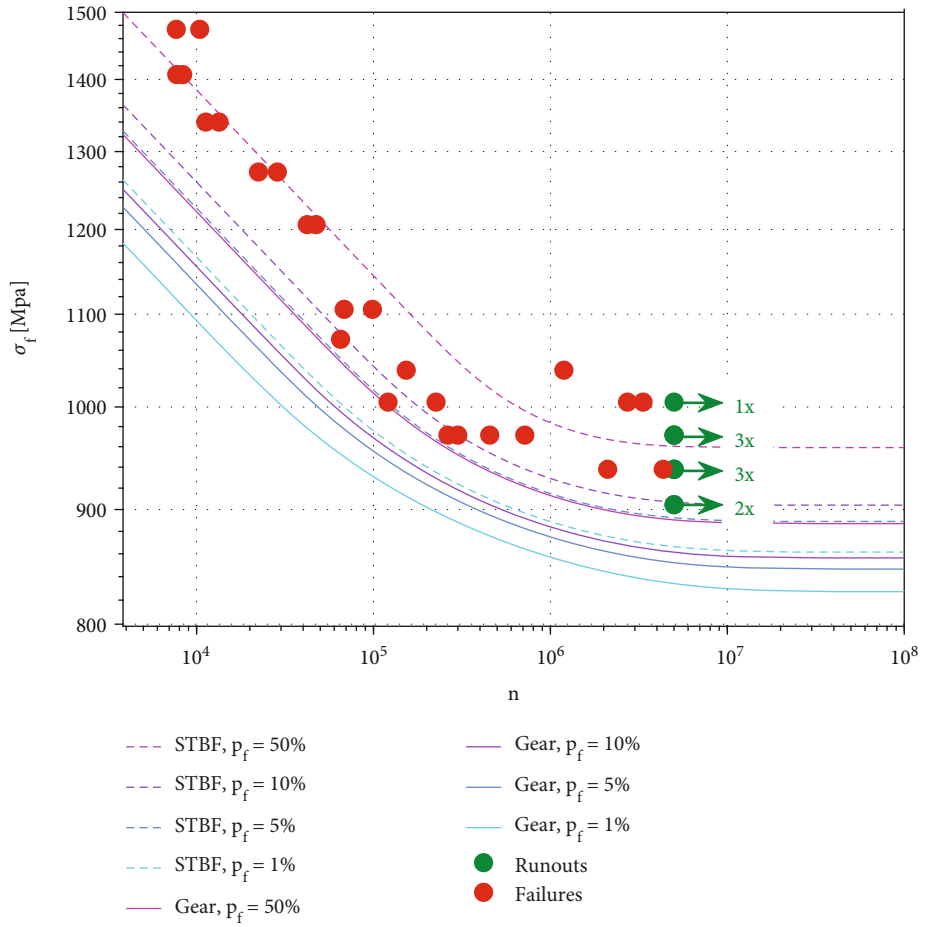

Figure 9: Comparison between STBF and gear SN curve at different failure probability.

has been stopped to the STBF one. However, as will be shown in the next section, it is possible to estimate the gear SN without losing any information.

4. Estimation of the Gear SN Curve

In order to estimate the gear SN curve, it is necessary to find a statistical relation between gear and teeth failure. This relation is based on the idea that, for the tooth root bending failure, a gear is considered failed when a single tooth breaks. The broken tooth will be the weakest one [36–38, 52, 53, 64].

By means of a mathematical passage [65], it is possible to use SoE in order to define the CDF of the minimum value observed over n extractions of X (the distribution of which is known) as follows:

$$F_{X_{(1)(x)}} = 1 - \left(1 - F_{X(x)}\right)^n, \tag{9}$$

where $F_{X(x)}$ is the smallest value distribution and $F_{X(x)}$ is the parent one. Figure 6 graphically explains Equation (9) effect: the smallest value distribution is narrower and with a lower scale parameter.

Accordingly, the gear CDF F_{gear} can be defined as the CDF of the weakest tooth among the z gear teeth, the CDF of which is F_{tooth}:

$$F_{\text{gear}} = 1 - (1 - F_{\text{tooth}})^z. \tag{10}$$

However, the CDF defined in the previous section (i.e., Equation (8)) does not describe the teeth themself but the STBF experimental data, in which the failed teeth is weakest one among the teeth pair. Therefore, Equation (10) can be rewritten as follows:

$$F_{\text{gear}} = 1 - (1 - F_{\text{STBF}})^{z/2}. \tag{11}$$

That is, F_{gear} is considered as a system of teeth pair, within which the smallest value over the $z/2$ teeth pair defines the gear load carrying capacity. In other words, the gear is considered as a system $z/2$ teeth pair among which the weakest pair rules the gear failure. Figure 7 reports the estimated gear PSN curve. Similarly, Figure 8 shows different SN, at different reliability level.

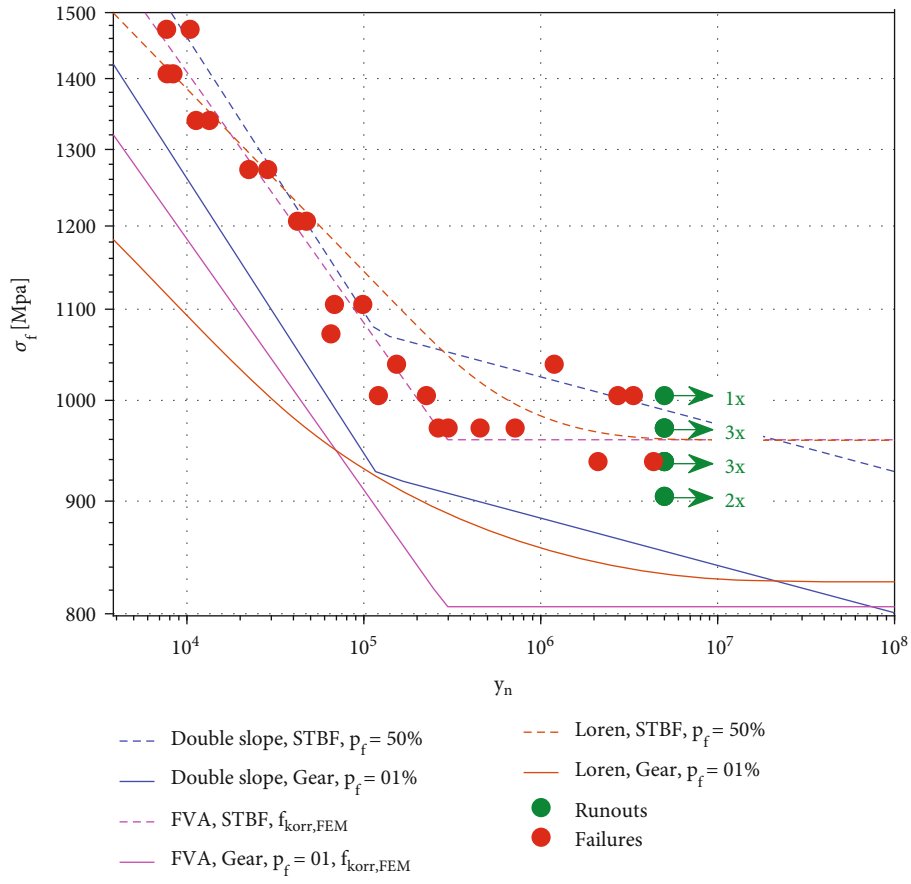

Figure 10: Comparison between various models.

5. Results and Conclusion

Figure 9 reports different SN curves, at different failure probabilities, for both the STBF and the gear case. It is possible to notice that, as already anticipated, the gear PDF results to be narrower that the teeth one; indeed, gear percentile is much closed than the teeth one (see Figure 6).

Looking at 50% percentile of the teeth SN curve (i.e., Figure 10), it is possible to observe, graphically, the effect of the combination of the two phenomena. At high stress level, the probability of having infinite life is close to zero; therefore, the predominant phenomena is the crack propagation. Here, the curve is a line that almost fits the data, as imposed by the model adopted in order to estimate the finite life region. On the other hand, at stress level almost close to the STF fatigue limit (e.g., around 1000 MPa), there is the compresence of both phenomena. Indeed, the curve at 50% failure probability passes in between those points failed by crack propagation (on the left) and those points failed because of load higher than the fatigue limit. Finally, at stress level close to the fatigue limit, the number of cycle to failure tends to the infinite life.

Figure 10 shows a comparison between curves; one has been estimated with the adopted model, and the other has been obtained from literature approaches. All the curves are coherent with each other.

The curves named "double slope" have been estimated according to [17, 18]. The one named "FVA, STBF" has been obtained by estimating the finite life behaviour by fit of experimental data; on the other hand, its long life one has been estimated by means of a staircase procedure. "FVA, Gear" has been obtained applying Sthal's corrective coefficient [39] on "FVA, STBF". All the curves adopt $f_{korr,FEM}$ in order to deal with the load difference effect.

Focusing on the limited life region of the STBF curves, results are similar. Furthermore, due to Equation (8) implication, in the region close to the STBF fatigue limit, the adopted model estimates a higher life because of the compresence of two failure mechanisms, one occurring at high number of cycles, one at lower number cycle. Indeed, both failure modes have a similar "weight." On the other hand, in the STBF long-life region, both endurance limit and the fatigue limit have the same value. This implies that the selected runout level is higher enough to represent the infinite life phenomena.

However, in the gear finite life region, it is possible to notice a difference between the estimated gear life. This different prediction is due to the different estimated variance, which is estimated with a higher value by the adopted Loren model. On the other hand, in the gear long-life region, the predicted gear life is in between the two curves. The

estimated gear fatigue limit at 1% probability of failure is slightly higher than the one predicted adopting the FVA coefficients. The reason behind is that the estimated variance is slightly lower than the ones adopted to calculate those coefficients.

6. Conclusions

A statistical framework, through which estimating the gear tooth root bending fatigue SN curve starting from STFB test data, is proposed here. The estimation framework has been developed considering a symmetric Single Tooth bending Fatigue (STBF) test configuration, and it is based on the hypothesis of fatigue limit existence.

STBF test results have been elaborated by means of a Maximum Likelihood (ML) model based on Murakami's idea of nonpropagating crack. Statistical consideration, based on statistic of extreme (SoE), has been adopted in order to estimate the gear SN curve.

The estimated curves have been compared with those obtained adopting other models. Results seem to be coherent. However, each estimation techniques have its own biases that result in a different estimation of the gear life.

It is worth underlying that a similar statistical framework can be developed in the case of an asymmetric STBF test configuration, where only one tooth is tested, by estimating the tooth SN curve with Equation (7) and using Equation (10).

Acronyms

CDF: Cumulative density function
ML: Maximum Likelihood
MG: Meshing gear
PDF: Probability density function
STBF: Single Tooth Bending Fatigue
SoE: Statistic of extreme
PSN: Probability-Stress-Number (of cycle).

Data Availability

The STBF test data supporting this article are from previously reported studies, which have been cited.

Conflicts of Interest

The authors declare that there is no conflict of interest regarding the publication of this paper.

Acknowledgments

The authors express their gratitude to Professor Stefano Beretta for his invaluable support during the validation of this statistical model.

References

[1] G. Henriot, *Ingranaggi, trattato teorico e pratico–volume 1–2 Edizione Italiana*, Tecniche Nuove, Milano, 1987.

[2] J. S. Morais and MAAG Gear Company Ltd., *Calculation and Practice of Gears, Gear Drives, Toothed Couplings and Synchronous Clutch Couplings*, MAAG GEAR BOOK, 1990.

[3] ISO-ISO/FDIS, "10825-1- Gears-wear and damage to gear teeth — part 1: terminology," 2021.

[4] ANSI/AGMA, "1010-F14 (R 2020) - Appearance of gear teeth-terminology of wear and failure," 2020.

[5] P. D. Samuel and D. J. Pines, "A review of vibration-based techniques for helicopter transmission diagnostics," *Journal of Sound and Vibration*, vol. 282, no. 1–2, pp. 475–508, 2005.

[6] D. Zhang, S. Liu, B. Liu, and J. Hong, "Investigation on bending fatigue failure of a micro-gear through finite element analysis," *Engineering Failure Analysis*, vol. 31, pp. 225–235, 2013.

[7] K. Feng, P. Borghesani, W. A. Smith et al., "Vibration-based updating of wear prediction for spur gears," *Wear*, vol. 426-427, pp. 1410–1415, 2019.

[8] F. Concli, L. Pierri, and C. Sbarufatti, "A model-based SHM strategy for gears—development of a hybrid FEM-analytical approach to investigate the effects of surface fatigue on the vibrational spectra of a back-to-back test rig," *Applied Sciences*, vol. 11, no. 5, p. 2026, 2021.

[9] S. Sendlbeck, A. Fimpel, B. Siewerin, M. Otto, and K. Stahl, "Condition monitoring of slow-speed gear wear using a transmission error-based approach with automated feature selection," *International Journal of Prognostics and Health Management*, vol. 12, no. 2, 2021.

[10] E. Conrado, P. C. Davoli, and K. Michaelis, "Recognizing gear failures," *Machine Design*, vol. 63, pp. 64–67, 2007.

[11] L. Bonaiti, A. B. M. Bayoumi, F. Concli, F. Rosa, and C. Gorla, "Gear root bending strength: a comparison between single tooth bending fatigue tests and meshing gears," *Journal of Mechanical Design*, vol. 143, no. 10, pp. 1–17, 2021.

[12] ISO 6336-3, "Calculation of load capacity of spur and helical gears — part 3: calculation of tooth bending strength," 2019.

[13] ANSI/AGMA 2001-D04, "Fundamental rating factors and calculation methods for involute spur and helical gear teeth," 2010.

[14] ISO 6336-6: 2019, "Calculation of load capacity of spur and helical gears, part 6: calculation of service life under variable load," ISO Technical Committee, Geneva, CH, 2019.

[15] ISO 6336-5: 2016, *Calculation of load capacity of spur and helical gears — part 5: strength and quality of materials*, 2016.

[16] M. Hein, M. Geitner, T. Tobie, K. Stahl, and B. Pinnekamp, *Reliability of Gears - Determination of Statistically Validated Material Strength Numbers*, American Gear Manufacturers Association Fall Technical Meeting 2018, 2018.

[17] L. Bonaiti and C. Gorla, "Estimation of gear SN curve for tooth root bending fatigue by means of maximum likelihood method and statistic of extremes," *International Journal of Fatigue*, vol. 153, p. 106451, 2021.

[18] L. Bonaiti, F. Rosa, P. M. Rao, F. Concli, and C. Gorla, "Gear root bending strength: statistical treatment of single tooth bending fatigue tests results: conference proceedings," *Forschung im Ingenieurwesen*, pp. 1–8, 2021.

[19] J. E. Spindel and E. Haibach, "Some considerations in the statistical determination of the shape of SN curves," in *Statistical analysis of fatigue data*, ASTM International, 1981.

[20] J. E. Spindel, B. R. Board, and E. Haibach, *The Statistical Analysis of Fatigue Test Results*, 1979.

[21] A. Fernández-Canteli, S. Blasón, B. Pyttel, M. Muniz-Calvente, and E. Castillo, "Considerations about the existence or non-

existence of the fatigue limit: implications on practical design," *International Journal of Fracture*, vol. 223, no. 1-2, pp. 189–196, 2020.

[22] B. Pyttel, D. Schwerdt, and C. Berger, "Very high cycle fatigue – is there a fatigue limit?," *International Journal of Fatigue*, vol. 33, no. 1, pp. 49–58, 2011.

[23] D. Fuchs, S. Schurer, T. Tobie, and K. Stahl, "A model approach for considering nonmetallic inclusions in the calculation of the local tooth root load-carrying capacity of high-strength gears made of high-quality steels," *Proceedings of the Institution of Mechanical Engineers, Part C: Journal of Mechanical Engineering Science*, vol. 233, no. 21–22, pp. 7309–7317, 2019.

[24] D. Fuchs, S. Rommel, T. Tobie, and K. Stahl, "Fracture analysis of fisheye failures in the tooth root fillet of high-strength gears made out of ultra-clean gear steels," *Forschung im Ingenieurwesen*, vol. 85, no. 4, pp. 1109–1125, 2021.

[25] D. Fuchs, S. Schurer, T. Tobie, and K. Stahl, "On the determination of the bending fatigue strength in and above the very high cycle fatigue regime of shot-peened gears," *Forschung im Ingenieurwesen*, vol. 86, no. 1, pp. 81–92, 2022.

[26] D. Fuchs, S. Schurer, T. Tobie, and K. Stahl, "Investigations into non-metallic inclusion crack area characteristics relevant for tooth root fracture damages of case carburised and shot-peened high strength gears of different sizes made of high-quality steels," *Forschung im Ingenieurwesen*, vol. 83, no. 3, pp. 579–587, 2019.

[27] D. Fuchs, S. Rommel, T. Tobie, and K. Stahl, "In-depth analysis of crack area characteristics of fisheye failures influenced by the multiaxial stress condition in the tooth root fillet of high-strength gears," *Proceedings of the Institution of Mechanical Engineers, Part C: Journal of Mechanical Engineering Science*, no. article 09544062211061674, 2021.

[28] S. Beretta and Y. Murakami, "Statistical analysis of defects for fatigue strength prediction and quality control of materials," *Fatigue and Fracture of Engineering Materials and Structures*, vol. 21, no. 9, pp. 1049–1065, 1998.

[29] Y. Murakami and S. Beretta, "Small defects and inhomogeneities in fatigue strength: experiments, models and statistical implications," *Extremes*, vol. 2, no. 2, pp. 123–147, 1999.

[30] Y. Murakami, "Mechanism of fatigue in the absence of defects and inclusions," in *Metal Fatigue: Effects of small defects and non-metallic inclusions*, pp. 1–11, Elsevier, UK, 2019.

[31] F. G. Pascual and W. Q. Meeker, "Estimating fatigue curves with the random fatigue-limit model," *Technometrics*, vol. 41, no. 4, pp. 277–289, 1999.

[32] S. Beretta, P. Clerici, and S. Matteazzi, "The effect of sample size on the confidence of endurance fatigue tests," *Fatigue and Fracture of Engineering Materials and Structures*, vol. 18, no. 1, pp. 129–139, 1995.

[33] S. Lorén, "Fatigue limit estimated using finite lives," *Fatigue and Fracture of Engineering Materials and Structures*, vol. 26, no. 9, pp. 757–766, 2003.

[34] S. Lorén and M. Lundström, "Modelling curved S–N curves," *Fatigue and Fracture of Engineering Materials and Structures*, vol. 28, no. 5, pp. 437–443, 2005.

[35] I. J. Hong, A. Kahraman, and N. Anderson, "An experimental evaluation of high-cycle gear tooth bending fatigue lives under fully reversed and fully released loading conditions with application to planetary gear sets," *Journal of Mechanical Design*, vol. 143, no. 2, 2021.

[36] S. B. Rao and D. R. McPherson, "Experimental characterization of bending fatigue strength in gear teeth," *Gear Technology*, vol. 20, no. 1, pp. 25–32, 2003.

[37] D. R. McPherson and S. B. Rao, *Methodology for Translating Single-Tooth Bending Fatigue Data to Be Comparable to Running Gear Data*, Gear Technology, 2008.

[38] H. Rettig, "Ermittlung von zahnfußfestigkeits-kennwerten auf verspannungsprüfständen und pulsatoren–vergleich der prüfverfahren und gewonnenen kennwerte," *Antriebstechnik*, vol. 26, pp. 51–55, 1987.

[39] K. Stahl, *Lebensdauerstatistik : Abschlussbericht : Forschungsvorhaben Nr. 304*, FVA, 1999.

[40] M. Benedetti, V. Fontanari, B.-R. Höhn, P. Oster, and T. Tobie, "Influence of shot peening on bending tooth fatigue limit of case hardened gears," *International Journal of Fatigue*, vol. 24, no. 11, pp. 1127–1136, 2002.

[41] F. Dobler, T. Tobie, and K. Stahl, "Influence of low temperatures on material properties and tooth root bending strength of case-hardened gears," in *Proceedings of the ASME 2015 International Design Engineering Technical Conferences and Computers and Information in Engineering Conference. Volume 10: ASME 2015 Power Transmission and Gearing Conference; 23rd Reliability, Stress Analysis, and Failure Prevention Conference*, Boston, Massachusetts, USA, 2015.

[42] T. Tobie and P. Matt, "Empfehlungen zur Vereinheitlichung von Tragfähigkeitsversuchen an vergüteten und gehärteten Zylinderrädern," Technical Report FVA-Richtlinie 563-I, 2012.

[43] L. Vilela Costa, D. de Oliveira, D. Wallace, V. Lelong, and K. O. Findley, "Bending fatigue in low-pressure carbonitriding of steel alloys with boron and niobium additions," *Journal of Materials Engineering and Performance*, vol. 29, no. 6, pp. 3593–3602, 2020.

[44] J. J. Spice, D. K. Matlock, and G. Fett, "Optimized carburized steel fatigue performance as assessed with gear and modified Brugger fatigue tests," *SAE Transactions*, vol. 111, pp. 589–597, 2002.

[45] D. J. Medlin, B. E. Cornelissen, D. K. Matlock, G. Krauss, and R. J. Filar, "Effect of thermal treatments and carbon potential on bending fatigue performance of SAE 4320 gear steel," *SAE Transactions*, vol. 108, pp. 547–556, 1999.

[46] D. R. McPherson and S. B. Rao, "Mechanical testing of gears," *Materials Park, OH: ASM International*, vol. 2000, pp. 861–872, 2000.

[47] E. Wildhaber, "Measuring tooth thickness of involute gears," *American Machinist*, vol. 59, p. 551, 1923.

[48] S SAE, *J 1619, Single tooth gear bending fatigue test*, SAE International, 2017.

[49] R. W. Buenneke, M. B. Slane, C. R. Dunham, M. P. Semenek, M. M. Shea, and J. E. Tripp, "Gear single tooth bending fatigue test," *SAE Transactions*, vol. 91, pp. 3266–3274, 1982.

[50] C. Gorla, E. Conrado, F. Rosa, and F. Concli, "Contact and bending fatigue behaviour of austempered ductile iron gears," *Proceedings of the Institution of Mechanical Engineers, Part C: Journal of Mechanical Engineering*, vol. 232, no. 6, pp. 998–1008, 2018.

[51] G. Gasparini, U. Mariani, C. Gorla, M. Filippini, and F. Rosa, *Bending fatigue tests of helicopter case carburized gears: influence of material, design and manufacturing parameters*, American Gear Manufacturers Association (AGMA) Fall Technical Meeting, 2008.

[52] I. Hong, Z. Teaford, and A. Kahraman, "A comparison of gear tooth bending fatigue lives from single tooth bending and rotating gear tests," *Forschung im Ingenieurwesen*, 2021.

[53] J. B. Seabrook and D. W. Dudley, "Results of a fifteen-year program of flexural fatigue testing of gear teeth," *Journal of Engineering for Industry*, vol. 86, no. 3, pp. 221–237, 1964.

[54] F. Concli, L. Maccioni, and L. Bonaiti, "Reliable gear design: translation of the results of single tooth bending fatigue tests through the combination of numerical simulations and fatigue criteria," *WIT Transactions on Engineering Sciences*, vol. 130, pp. 111–122, 2021.

[55] F. Concli, L. Maccioni, L. Fraccaroli, and L. Bonaiti, "Early crack propagation in single tooth bending fatigue: combination of finite element analysis and critical-planes fatigue criteria," *Metals*, vol. 11, no. 11, p. 1871, 2021.

[56] C. Gorla, F. Rosa, E. Conrado, and F. Concli, "Bending fatigue strength of case carburized and nitrided gear steels for aeronautical applications," *International Journal of Applied Engineering Research*, vol. 12, no. 21, pp. 11306–11322, 2017.

[57] C. Gorla, F. Rosa, F. Concli, and H. Albertini, "Bending fatigue strength of innovative gear materials for wind turbines gearboxes: effect of surface coatings," in *Proceedings of the ASME 2012 International Mechanical Engineering Congress and Exposition. Volume 7: Fluids and Heat Transfer, Parts A, B, C, and D*, pp. 3141–3147, Houston, Texas, USA, 2012.

[58] C. Gorla, F. Rosa, E. Conrado, and H. Albertini, "Bending and contact fatigue strength of innovative steels for large gears," *Proceedings of the Institution of Mechanical Engineers, Part C: Journal of Mechanical Engineering Science*, vol. 228, no. 14, pp. 2469–2482, 2014.

[59] L. Bonaiti, F. Concli, C. Gorla, and F. Rosa, "Bending fatigue behaviour of 17-4 PH gears produced via selective laser melting," *Procedia Structural Integrity*, vol. 24, 2019.

[60] F. Concli, L. Bonaiti, R. Gerosa et al., "Bending fatigue behavior of 17-4 ph gears produced by additive manufacturing," *Applied Sciences*, vol. 11, no. 7, p. 3019, 2021.

[61] S. Colombo, *Advanced Statistical Models for Bending Fatigue Characterization of Gears*, Politecnico di Milano, 2019.

[62] W. B. Nelson, *Applied Life Data Analysis, vol. 521*, John Wiley & Sons, 2003.

[63] W. B. Nelson, *Accelerated Testing: Statistical Models, Test Plans, and Data Analysis, vol. 344*, John Wiley & Sons, 2009.

[64] M. Li, L. Y. Xie, H. Y. Li, and J. G. Ren, "Life distribution transformation model of planetary gear system," *Chinese Journal of Mechanical Engineering*, vol. 31, no. 2, pp. 1–8, 2018.

[65] S. Beretta, *Affidabilità delle costruzioni meccaniche: Strumenti e metodi per l'affidabilità di un progetto*, Springer Science & Business Media, 2010.